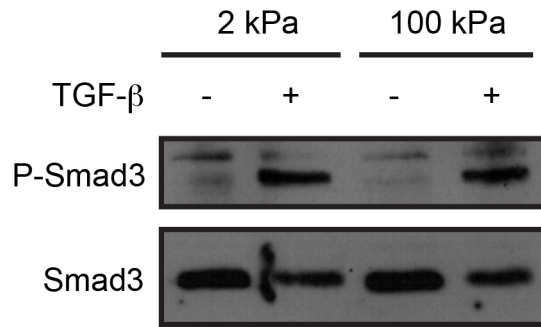


## SUPPLEMENTAL INFORMATION

**Supplemental Table 1**

| <b>Primer</b>  | <b>Primer Sequence</b>  |
|----------------|-------------------------|
| ACTA2 Forward  | ACGCGAAGCTCGTTATAGAAG   |
| ACTA2 Reverse  | GACCCTGAAGTATCCGATAGAAC |
| COL1A1 Forward | GAACAAGGTGACAGAGGCATA   |
| COL1A1 Reverse | GAGAACCAGCAGAGCCA       |
| COL3A1 Forward | CATTGCGTCCATCAAAGCC     |
| COL3A1 Reverse | GAAAGGATGGAGAGTCAGGAA   |
| COL4A1 Forward | GTTACCTTTCTCTCCATATCCTG |
| COL4A1 Reverse | GGACAGGCACAAGTTAAGGAA   |
| GAPDH Forward  | GTAACCAGGCGTCCGATAC     |
| GAPDH Reverse  | TCTCTGCTCCTCCCTGTTC     |
| PAI1 Forward   | TTCCCAAAGACCAGAACCAG    |
| PAI1 Reverse   | GCAACAAGAGCCAATCACAAG   |
| TAZ Forward    | GCGTGCCCAGAAAGATGAA     |
| TAZ Reverse    | AGGATCTTTTTCCGCCACGA    |
| YAP Forward    | AAGACACTGCATTCTGAGTCC   |
| YAP Reverse    | GAATATCAATCCCAGCACAGC   |

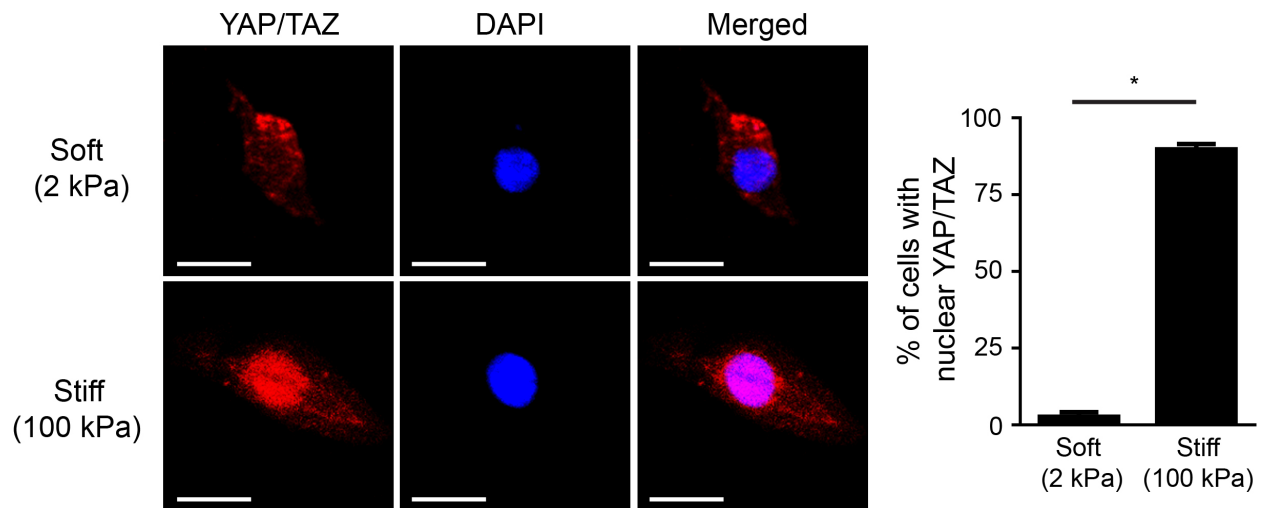
### Supplemental Figure 1



**Supplemental Figure 1: TGF- $\beta$ -induced Smad3 phosphorylation is unaffected by matrix stiffness.**

NRK49F rat renal fibroblasts cultured on soft (2 kPa) and stiff (100 kPa) fibronectin-coated gels were stimulated with TGF- $\beta$  10 ng/mL for 30 mins, followed by analysis of Smad3 phosphorylation. Phospho-Smad3 has previously been shown to run as a double band<sup>1,2</sup>. The blot shown is representative of n = 3 replicates.

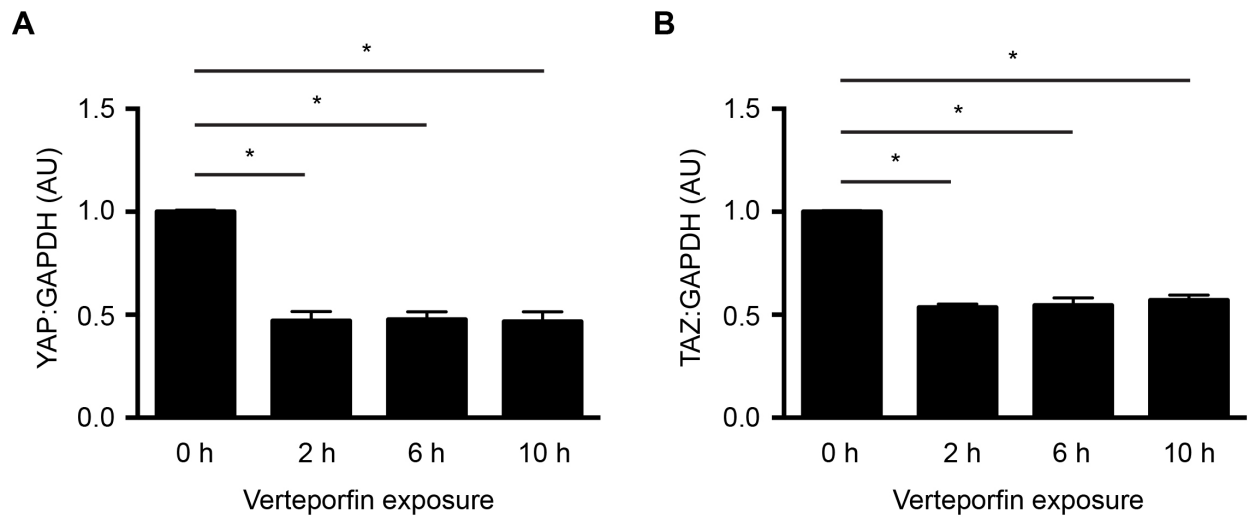
## Supplemental Figure 2



**Supplemental Figure 2: The localization of YAP/TAZ in cultured fibroblasts is regulated by ECM stiffness.**

NRK49F fibroblasts cultured on soft (2 kPa) or stiff (100 kPa) fibronectin-coated gels were immunostained with antibody recognizing YAP and TAZ (red). Nuclei (blue) were counterstained with DAPI. Scale bar: 20  $\mu\text{m}$ . The percentage of cells with predominantly nuclear YAP/TAZ staining was quantified as described in the Methods section (n = 3 replicates/condition). Student's t test was performed. \* p < 0.05.

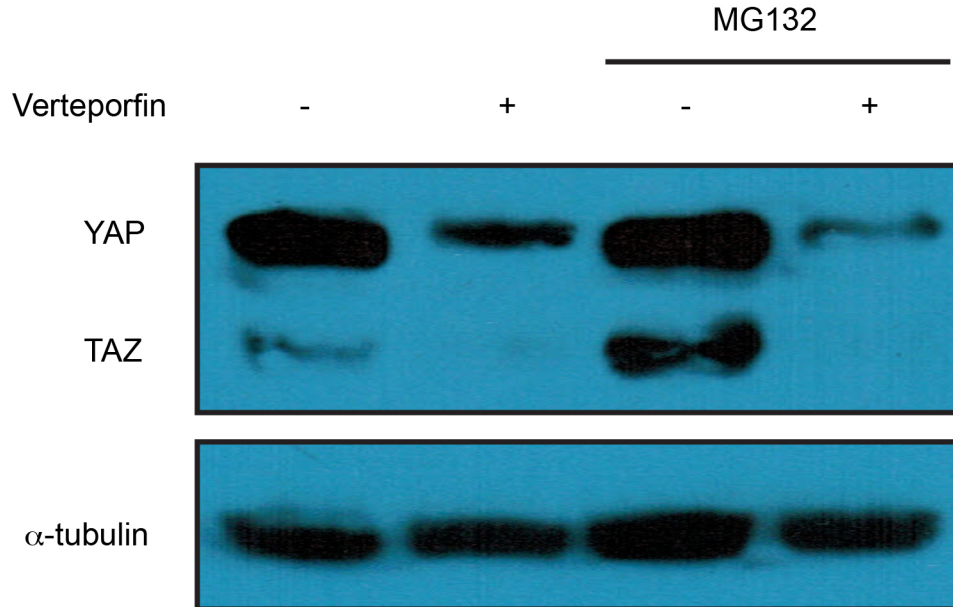
### Supplemental Figure 3



### Supplemental Figure 3: Verteporfin treatment of NRK49F rat renal fibroblasts results in reduced YAP and TAZ mRNA levels.

NRK49F renal fibroblasts were treated for verteporfin for the indicated times. RNA was then harvested, reverse transcribed, and quantitative reverse transcription PCR performed to assess YAP and TAZ mRNA levels. Results are representative of n = 3 independent replicates per time point. \* p < 0.05.

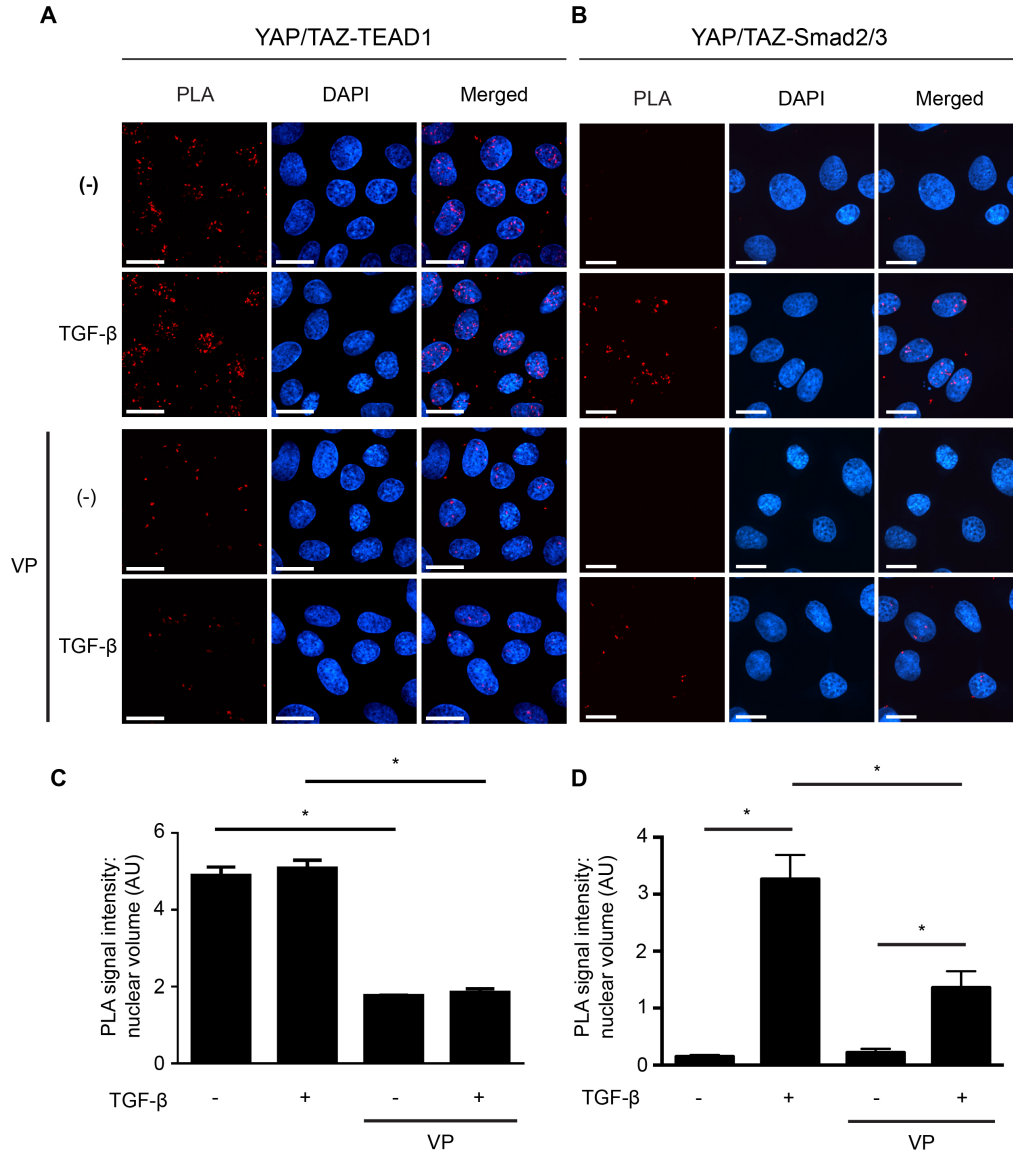
## Supplemental Figure 4



### Supplemental Figure 4: Verteporfin does not enhance the proteasomal degradation of YAP and TAZ.

NRK49F fibroblasts were treated with or without MG132 10  $\mu$ mol/L for 1 h to block the proteasome, followed by verteporfin 250 nmol/L for 2 h. Cell lysates were immunoblotted for YAP, TAZ, and  $\alpha$ -tubulin. The blot shown is representative of n = 3 experiments.

## Supplemental Figure 5

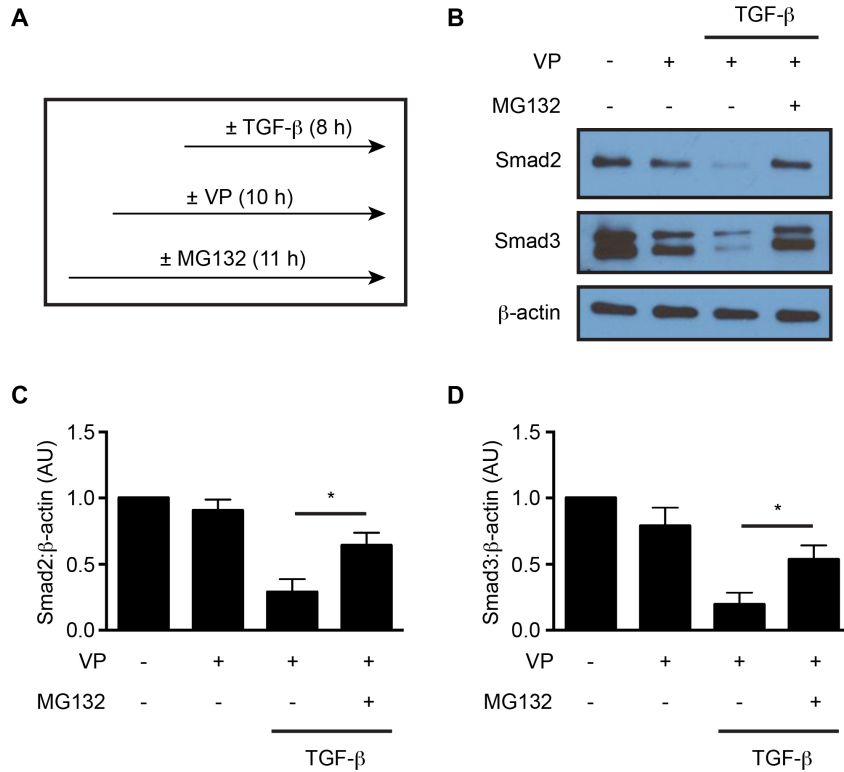


### Supplemental Figure 5: YAP/TAZ inhibition with verteporfin reduces YAP/TAZ-dependent protein interactions.

NRK49F fibroblasts grown on fibronectin-coated glass coverslips were treated with or without verteporfin (VP) 250 nmol/L for 2 hours, followed by TGF- $\beta$  10 ng/mL for 30 minutes, and then subjected to proximity ligation assays (PLA) to detect (A) YAP/TAZ-TEAD1 and (B) YAP/TAZ-Smad2/3 interactions (red fluorescence). Cells were counterstained with DAPI to

identify nuclei. Scale bar: 15  $\mu\text{m}$ . The mean red fluorescence intensity normalized to nuclear volume was quantified in a minimum of 300 cells per condition, as a measure of (C) nuclear YAP/TAZ-TEAD1 and (D) nuclear Smad2/3-YAP/TAZ interaction. One-way ANOVA with post-hoc Fisher's least significant difference was performed. \*  $p < 0.05$ . Abbreviations: AU, arbitrary units.

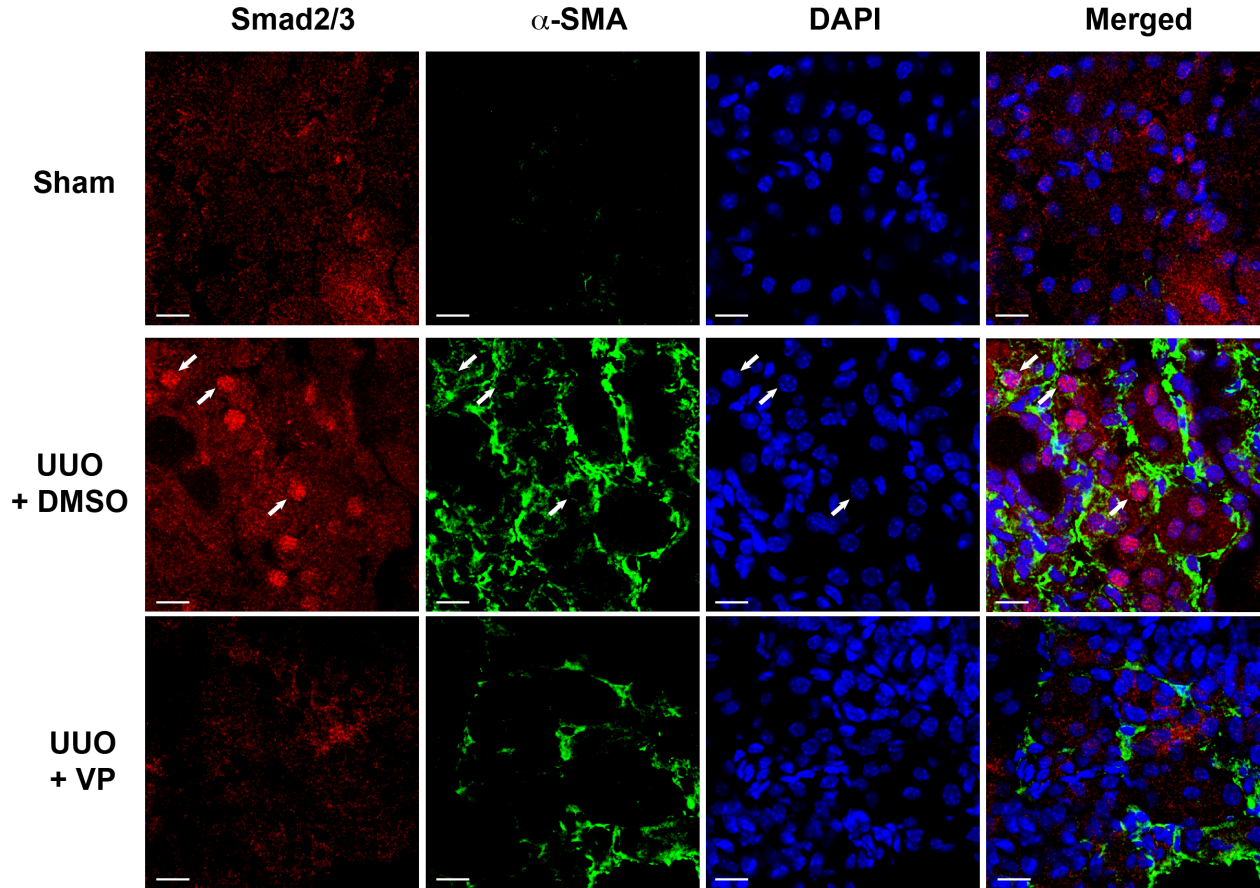
## Supplemental Figure 6



### Supplemental Figure 6: Verteporfin enhances the proteasomal degradation of Smad2 and Smad3 following TGF-β stimulation.

(A) NRK49F fibroblasts grown in fibronectin-coated plastic wells were treated with or without MG132 10  $\mu\text{mol/L}$  for 1 h to block the proteasome, followed by 2 h of verteporfin (VP) 250 nmol/L, and then TGF- $\beta$  10 ng/mL for 8 h. Cell lysates were immunoblotted for Smad2, Smad3, and  $\beta$ -actin. Representative blots from  $n = 4$  independent experiments are shown in (B). Smad3 has previously been reported to have doublet staining<sup>3</sup>. Quantification of (C) Smad2 and (D) Smad3 relative to  $\beta$ -actin demonstrating that prolonged exposure to VP and TGF- $\beta$  leads to diminished Smad2/3 levels, with proteasomal inhibition resulting in a partial rescue of Smad2 and Smad3. \*  $p < 0.05$ . Abbreviations: AU, arbitrary units.

## Supplemental Figure 7



**Supplemental Figure 7: Nuclear accumulation of Smad2/3 in the obstructed kidney is attenuated by verteporfin treatment.**

Mice undergoing sham surgery (n = 6) or unilateral ureteral obstruction were treated with verteporfin (n = 7) or DMSO control (n = 9), beginning immediately after surgery. Frozen kidney sections were stained with antibodies directed against Smad2/3 and  $\alpha$ -smooth muscle actin ( $\alpha$ -SMA), and nuclei were counterstained with DAPI. Shown are representative images. Prominent interstitial  $\alpha$ -SMA staining and nuclear Smad2/3 accumulation was observed in DMSO-treated UUO mice. In sharp contrast, VP-treated UUO kidneys displayed attenuated  $\alpha$ -SMA staining, and little if any nuclear Smad2/3. White arrows depict interstitial  $\alpha$ -SMA<sup>+</sup> interstitial cells with predominantly nuclear Smad2/3 staining. Scale bar: 20  $\mu$ m.

## **COMPLETE METHODS**

### **Polyacrylamide and silicone gel preparation**

Glass coverslips were coated with polyacrylamide hydrogels as previously reported <sup>4,5</sup>. Briefly, acrylamide and bisacrylamide were mixed at pre-defined ratios to generate gels of 2 kPa and 100 kPa stiffness. To provide a biologically relevant surface for fibroblasts to adhere to, hydrogels were treated with 500 µl of the cross-linking chemical sulfo-SANPAH (Sigma-Aldrich, Oakville, Ontario, Canada). Sulfo-SANPAH cross-linking was then activated by exposing the dish to UV radiation for 10 minutes. Unbound sulfo-SANPAH was then washed away with HEPES buffer, and sterile fibronectin 10 µg/mL (YO Proteins AB, Huddinge, Sweden) added to create a uniform, thin layer of extracellular matrix protein for cell adhesion.

Silicone gels were prepared as previously reported <sup>6</sup>. Briefly, polydimethyl silicone (PDMS) base (Dow Corning, Mississauga, Ontario, Canada) was mixed with curing agent at pre-determined ratios generating gels of 2 kPa and 100 kPa stiffness. Polymer was poured into 35 mm and 100 mm petri dishes, or glass chamber slides. Silicone gels were allowed to polymerize at 65°C for 4 days <sup>7,8</sup>, and then coated with sterile fibronectin 10 µg/ml overnight by passive adsorption at 37°C.

### **Cell culture and treatments**

Immortalized normal rat kidney interstitial fibroblasts (NRK49F) and primary human dermal fibroblasts were purchased from ATCC (Manassas, VA) and Lonza (Mississauga, Ontario, Canada) respectively. Cells were cultured at 37°C with 5% CO<sub>2</sub> and grown in Dulbecco's

Modified Eagle Medium (DMEM) with 5% or 10% Fetal Bovine Serum (FBS). Following overnight serum deprivation (DMEM + 1% FBS), cells grown on human fibronectin-coated soft gels, stiff gels, or plastic substrates were stimulated with TGF- $\beta$  10 ng/mL (R&D Systems, Minneapolis, MN) and/or verteporfin (Sigma-Aldrich) for the indicated times. Verteporfin treatment concentration was 250 nmol/L, unless otherwise indicated. In some experiments, cells were treated with MG132 10  $\mu$ mol/L (Sigma-Aldrich) to inhibit the 26S proteasome. Cells were cultured in the dark, and ambient light exposure was minimized to avoid photoactivation of verteporfin.

### **Immunofluorescence staining**

NRK49F fibroblasts were cultured on human fibronectin-coated gels and glass coverslips as indicated for a minimum of 24 hours. Following treatments as indicated in the text, cells were fixed in 4% paraformaldehyde, permeabilized, and incubated with mouse anti-human YAP/TAZ antibody (Santa Cruz, cat no. sc-101199, Dallas, TX), rabbit anti-human Smad2 antibody (Cell Signaling, cat. no. 5339, Danvers, MA), or mouse anti-human Smad2/3 antibody (Cell Signaling, cat no. 8685). Primary antibodies were detected with CF555-conjugated donkey anti-mouse (Biotium, cat no. 20037, Hayward, CA), Alexa 488-conjugated donkey anti-mouse (Jackson ImmunoResearch, cat. no. 715-545-150, West Grove, PA), or CF647-conjugated donkey anti-rabbit IgG (Biotium, cat. no. 20047), followed by nuclear counterstaining with DAPI. Images were obtained using a WAVE FX-X1 spinning disk confocal microscope system (Quorum Technologies, Guelph, Ontario, Canada) or a Zeiss LSM 700 Inverted Confocal microscope (Carl Zeiss Canada, North York, Ontario, Canada)<sup>9, 10</sup>. The percentage of cells with predominantly nuclear YAP/TAZ or Smad2/3 was calculated using a modified published

protocol<sup>11</sup>. Briefly, mean staining intensity of either YAP/TAZ or Smad2/3 was digitally quantified using ImageJ (NIH, Bethesda, MD), with regions of interest placed around both the entire cell and the nucleus. Analysis was performed on cross-sectional images cut through the nucleus at its largest cross-sectional area. Cells with a nuclear:cellular staining ratio of  $\geq 1.6$  were deemed to have predominantly nuclear staining. A minimum of 50 cells per coverslip were examined per replicate.

### **Immunoblotting**

Cell lysates were separated by SDS-PAGE, and following transfer, membranes were blotted with the following primary antibodies: Smad2 (Cell Signaling, cat. no. 5339), Smad3 (Cell Signaling, cat. no. 9513S and 9523S), Smad2/3 (Cell Signaling, cat. no. 3102), phospho-Smad2 (Cell Signaling, cat. no. 3101), phospho-Smad3 (Cell Signaling, cat. no. 9520), YAP/TAZ (Santa Cruz, cat. no. sc-101199 and Cell Signaling, cat. no. 8418), alpha-tubulin (Sigma-Aldrich, cat. no. T-5618), GAPDH (Abcam, cat. no. 9482, Cambridge, UK), and  $\beta$ -actin (Sigma-Aldrich, cat. no. A1978). Primary antibodies were detected with horseradish peroxidase-conjugated donkey anti-rabbit (cat. no. 711-035-152), donkey anti-mouse (cat. no. 715-035-150), and donkey anti-goat (cat. no. 705-035-003) secondary antibodies (Jackson ImmunoResearch). Alpha-tubulin,  $\beta$ -actin, or GAPDH were the housekeeping proteins used for normalization. Quantitative analysis of band intensity was performed using ImageJ.

### **Transfection and luciferase reporter assay**

Fibroblasts grown on human fibronectin-coated soft (2 kPa), stiff (100 kPa), or plastic substrates were serum starved in DMEM + 1% FBS overnight, and then transfected with a Firefly

luciferase reporter construct driven by tandem Smad-binding element (SBE) consensus motifs, along with a control Renilla luciferase vector constitutively driven by the HSV-thymidine kinase promoter (Promega, Madison, WI). Transfected fibroblasts were stimulated with TGF- $\beta$  10 ng/mL and both Firefly and Renilla luminescence read 24 h later using a *Dual-Glo® Luciferase* kit and luminometer (Promega)<sup>12</sup>. In some experiments, cells were treated with verteporfin at the indicated concentrations. Smad transcriptional activity was calculated as the Firefly:Renilla luminescence ratio.

### **YAP silencing**

Following serum deprivation in DMEM + 2% FBS for 4 hours, NRK49F fibroblasts cultured in human fibronectin-coated plastic wells were transfected with 10 nmol/L of siRNA directed against YAP1 (Invitrogen, cat. no. SR505344, Carlsbad, CA) or a scrambled siRNA, using Lipofectamine RNAiMAX (Invitrogen). Forty eight hours after transfection, YAP silencing was confirmed via immunoblotting and cells were used for experiments.

### **Quantitative reverse transcription PCR**

Following various treatments as outlined in the text, RNA was collected from NRK49F fibroblasts, reverse transcribed, and levels of COL1A1, COL3A1, COL4A1, ACTA2, PAI1, TAZ, YAP, and GAPDH were quantified. Primer sequences are summarized in Supplemental Table 1. Experiments were performed in triplicate. Data analyses were performed using the Applied Biosystems Comparative CT method. All values were referenced to the mRNA transcript levels of the housekeeper gene GAPDH.

### **Proximity ligation assay**

NRK49F fibroblasts cultured on human fibronectin-coated glass coverslips were treated with or without verteporfin 250 nmol/L for 2 h, followed by TGF- $\beta$  10 ng/mL for 30 min. Cells were then subjected to Duolink<sup>TM</sup> proximity ligation assays as per the manufacturer's instructions (Olink Bioscience, Uppsala, Sweden)<sup>13</sup>. Briefly, cells were incubated with mouse anti-human YAP/TAZ (Santa Cruz, cat. no. sc-101199) and rabbit anti-human Smad2/3 (Cell Signaling, cat. no. 8685) primary antibodies or mouse anti-human YAP/TAZ (Santa Cruz, cat. no. sc-101199) and rabbit anti-TEAD1 primary antibodies (BD Biosciences, cat. no. 610922, Mississauga, Ontario, Canada). Proximity of YAP/TAZ to Smad2/3 or TEAD1 was detected by the addition of anti-mouse PLUS and anti-rabbit MINUS PLA probes, followed by ligation, rolling circle amplification, and hybridization with fluorescently labeled oligonucleotides. Fluorescent spots were detected by a WAVE FX-X1 spinning disk confocal microscope system (Quorum Technologies), and quantified as nuclear PLA signal intensity divided by nuclear volume. A minimum of 300 cells were counted per condition.

### **Animals and unilateral ureteral obstruction surgery**

#### *Study 1*

To assess YAP/TAZ localization in  $\alpha$ -smooth muscle actin<sup>+</sup> renal fibroblasts, male C57BL/6 mice (6 – 8 weeks old) were purchased from Jackson Laboratory (Bar Harbor, ME), and underwent either left-sided unilateral ureteral obstruction (UUO, n = 4) or sham surgery (n = 3). Briefly, a left-sided flank incision was made in anesthetized mice, and the left kidney and ureter identified. The left ureter was then obstructed with two 4-0 silk suture ties just distal to the renal pelvis. Seven days after surgery, mice were sacrificed and the left kidneys harvested, immersion

fixed in 10% neutral buffered formalin, and embedded in paraffin.

*Study 2 (UUO – early verteporfin treatment)*

To examine whether early verteporfin treatment could prevent renal fibrosis, male C57BL/6 mice (6 – 8 weeks old, Jackson Laboratory) underwent either left-sided UUO (n = 16) or sham surgery (n = 6). Mice undergoing UUO surgery were randomized to receive every other day intra-peritoneal injections of either verteporfin 100 mg/kg dissolved in 10% DMSO (n = 7) or DMSO vehicle control (n = 9). Treatment began immediately after surgery (day 0), and was continued until study end, 7 days after surgery.

*Study 3 (UUO – late verteporfin treatment)*

To examine whether late verteporfin treatment could prevent the progression of established fibrosis, male C57BL/6 mice (6 – 8 weeks old, Jackson Laboratory) underwent left-sided UUO (n = 17) or sham surgery (n = 4). Mice undergoing UUO surgery were randomized to receive intra-peritoneal injections of either verteporfin 100 mg/kg (n = 10) or DMSO vehicle (n = 7) as described for Study 2. Treatment in this study, however, began on day 7 post-UUO, a time point when renal fibrosis is already established in the obstructed left kidney, and was continued for a further 7 days. All mice were sacrificed 14 days after UUO or sham surgery.

**Tissue collection, preparation, and histology**

At study end, the left kidneys of all mice were harvested, and samples of each kidney were immersion fixed in 10% neutral buffered formalin or embedded in cryostat matrix (Tissue-Tek, VWR, Mississauga, Ontario, Canada). Frozen kidney sections were fixed in 4%

paraformaldehyde in phosphate-buffered saline, and stained with antibodies directed against Smad2/3 (Cell Signaling, cat. no. 8685) and  $\alpha$ -smooth muscle actin (Sigma-Aldrich, cat. no. A2547). The secondary antibodies used were CF647 donkey anti-rabbit IgG (Biotium, 1:1000) and CF555 donkey anti-mouse IgG (Biotium, 1:1000). Nuclei were counterstained with DAPI (1  $\mu$ g/ml). Images were taken with a WAVE FX-X1 spinning disk confocal microscope system (Quorum Technologies) using Volocity software (Perkin-Elmer, Woodbridge, ON, Canada). Formalin-fixed tissues were embedded in paraffin and sectioned before staining with picosirius red (Sigma-Aldrich) or antibodies against  $\alpha$ -smooth muscle actin (Dako, cat. no. M085129-2, Burlington, Ontario, Canada), YAP/TAZ (Cell Signaling, cat no. 8418), and type IV collagen (Cedarlane, cat. no. CL50411AP, Burlington, Ontario, Canada)<sup>14-16</sup>. In some experiments, serially cut sections were used for co-localization analysis. Stained sections were digitally scanned with an Aperio Scanscope XT scanner (Leica Biosystems, Concord, Ontario, Canada) and whole kidney staining (excluding the renal pelvis) analyzed using Aperio Imagescope software as previously described<sup>14-16</sup>.

### ***In situ* hybridization**

For generating digoxigenin (DIG) labeled antisense probe for *Ctgf*, a cDNA clone (MGC:8122, IMAGE:3589136) in pCMV-SPORT6 was linearized by EcoRI and 1  $\mu$ g of the linearized plasmid DNA was used as a template for *in vitro* transcription with T7 RNA polymerase (10881767001, Roche, Mississauga, Ontario, Canada) and DIG RNA Labeling Mix (11277073910, Roche). *In situ* hybridization was performed on formalin-fixed, paraffin-embedded mouse kidney sections as previously described<sup>17</sup> and the hybridized antisense probe

was visualized with alkaline phosphatase-conjugated anti-digoxigenin (11093274910, Roche) and BM purple AP substrate (11442074001, Roche).

### **Statistics**

A minimum of 3 independent experiments was performed for all *in vitro* studies. Data presented are mean  $\pm$  standard error of the mean (SEM). Between-group differences were measured using one-way ANOVA with Fisher's least significant difference post-hoc analysis where appropriate. Statistical analysis was performed using Graphpad Prism for Mac 6.0 (Graphpad Software, San Diego, CA).

### **Study approval**

All animal studies were approved by the St. Michael's Hospital Animal Ethics Committee, and conformed to the Canadian Council on Animal Care guidelines.

## REFERENCES

1. Finnson, KW, Tam, BY, Liu, K, Marcoux, A, Lepage, P, Roy, S, Bizet, AA & Philip, A: Identification of CD109 as part of the TGF-beta receptor system in human keratinocytes. *FASEB J* 20: 1525-1527, 2006.
2. Liu, C, Gaca, MD, Swenson, ES, Vellucci, VF, Reiss, M & Wells, RG: Smads 2 and 3 are differentially activated by transforming growth factor-beta (TGF-beta ) in quiescent and activated hepatic stellate cells. Constitutive nuclear localization of Smads in activated cells is TGF-beta-independent. *J Biol Chem* 278: 11721-11728, 2003.
3. Thien, A, Prentzell, MT, Holzwarth, B, Klasener, K, Kuper, I, Boehlke, C, Sonntag, AG, Ruf, S, Maerz, L, Nitschke, R, Grellscheid, SN, Reth, M, Walz, G, Baumeister, R, Neumann-Haefelin, E & Thedieck, K: TSC1 activates TGF-beta-Smad2/3 signaling in growth arrest and epithelial-to-mesenchymal transition. *Dev Cell* 32: 617-630, 2015.
4. Tse, JR & Engler, AJ: Preparation of hydrogel substrates with tunable mechanical properties. *Current protocols in cell biology / editorial board, Juan S. Bonifacino ... [et al.]* Chapter 10: Unit 10 16, 2010.
5. Kadow, CE, Georges, PC, Janmey, PA & Beningo, KA: Polyacrylamide hydrogels for cell mechanics: steps toward optimization and alternative uses. *Methods Cell Biol* 83: 29-46, 2007.
6. Godbout, C, Follonier Castella, L, Smith, EA, Talele, N, Chow, ML, Garonna, A & Hinz, B: The mechanical environment modulates intracellular calcium oscillation activities of myofibroblasts. *PLoS One* 8: e64560, 2013.

7. Goffin, JM, Pittet, P, Csucs, G, Lussi, JW, Meister, JJ & Hinz, B: Focal adhesion size controls tension-dependent recruitment of alpha-smooth muscle actin to stress fibers. *J Cell Biol* 172: 259-268, 2006.
8. Wipff, PJ, Rifkin, DB, Meister, JJ & Hinz, B: Myofibroblast contraction activates latent TGF-beta1 from the extracellular matrix. *J Cell Biol* 179: 1311-1323, 2007.
9. Chaturvedi, S, Yuen, DA, Bajwa, A, Huang, YW, Sokollik, C, Huang, L, Lam, GY, Tole, S, Liu, GY, Pan, J, Chan, L, Sokolsky, Y, Puthia, M, Godaly, G, John, R, Wang, C, Lee, WL, Brumell, JH, Okusa, MD & Robinson, LA: Slit2 prevents neutrophil recruitment and renal ischemia-reperfusion injury. *J Am Soc Nephrol* 24: 1274-1287, 2013.
10. Tole, S, Mukovozov, IM, Huang, YW, Magalhaes, MA, Yan, M, Crow, MR, Liu, GY, Sun, CX, Durocher, Y, Glogauer, M & Robinson, LA: The axonal repellent, Slit2, inhibits directional migration of circulating neutrophils. *J Leukoc Biol* 86: 1403-1415, 2009.
11. Fan, L, Sebe, A, Peterfi, Z, Masszi, A, Thirone, AC, Rotstein, OD, Nakano, H, McCulloch, CA, Szaszi, K, Mucsi, I & Kapus, A: Cell contact-dependent regulation of epithelial-myofibroblast transition via the rho-rho kinase-phospho-myosin pathway. *Mol Biol Cell* 18: 1083-1097, 2007.
12. Masszi, A, Speight, P, Charbonney, E, Lodyga, M, Nakano, H, Szaszi, K & Kapus, A: Fate-determining mechanisms in epithelial-myofibroblast transition: major inhibitory role for Smad3. *J Cell Biol* 188: 383-399, 2010.
13. Nilsson, I, Bahram, F, Li, X, Gualandi, L, Koch, S, Jarvius, M, Soderberg, O, Anisimov, A, Kholova, I, Pytowski, B, Baldwin, M, Yla-Herttuala, S, Alitalo, K, Kreuger, J & Claesson-Welsh, L: VEGF receptor 2/-3 heterodimers detected in situ by proximity ligation on angiogenic sprouts. *EMBO J* 29: 1377-1388, 2010.

14. Yuen, DA, Connelly, KA, Advani, A, Liao, C, Kuliszewski, MA, Trogadis, J, Thai, K, Advani, SL, Zhang, Y, Kelly, DJ, Leong-Poi, H, Keating, A, Marsden, PA, Stewart, DJ & Gilbert, RE: Culture-modified bone marrow cells attenuate cardiac and renal injury in a chronic kidney disease rat model via a novel antifibrotic mechanism. *PLoS One* 5: e9543, 2010.
15. Yuen, DA, Connelly, KA, Zhang, Y, Advani, SL, Thai, K, Kabir, G, Kepecs, D, Spring, C, Smith, C, Batruch, I, Kosanam, H, Advani, A, Diamandis, E, Marsden, PA & Gilbert, RE: Early outgrowth cells release soluble endocrine antifibrotic factors that reduce progressive organ fibrosis. *Stem Cells* 31: 2408-2419, 2013.
16. Zhang, Y, Yuen, DA, Advani, A, Thai, K, Advani, SL, Kepecs, D, Kabir, MG, Connelly, KA & Gilbert, RE: Early-outgrowth bone marrow cells attenuate renal injury and dysfunction via an antioxidant effect in a mouse model of type 2 diabetes. *Diabetes* 61: 2114-2125, 2012.
17. Wilkinson, DG: RNA detection using non-radioactive in situ hybridization. *Curr Opin Biotechnol* 6: 20-23, 1995.